Journal of Instrumentation

SISSA

PAPER • OPEN ACCESS

Design of beam optics for a Super Tau-Charm Factory

To cite this article: J.Q. Lan *et al* 2021 *JINST* **16** T07001

PUBLISHED BY IOP PUBLISHING FOR SISSA MEDIALAB

RECEIVED: *January 18, 2021*
REVISED: *March 29, 2021*
ACCEPTED: *April 23, 2021*
PUBLISHED: *July 2, 2021*

TECHNICAL REPORT

Design of beam optics for a Super Tau-Charm Factory

J.Q. Lan,[a,1] Q. Luo,[b,1] C. Zhang,[b] W.W. Gao,[a,*] Y. Xu[a] and Y. Bai[a]

[a] *School of Electronic, Electrical Engineering and Physics, Fujian University of Technology, Fuzhou 350118, China*
[b] *National Synchrotron Radiation Laboratory, University of Science and Technology of China, Hefei 230026, China*

E-mail: gaoww@ustc.edu.cn

ABSTRACT: Beam optics design for a Super Tau-Charm Factory (STCF) that planning in China is presented in this paper. This STCF is an electron-positron circular collider characterized with high luminosity, wide energy ranges as well as high longitudinally polarized electron beam. In order to achieve high luminosity, the recently proposed collision scheme based on large Piwinski angle and crab waist sextupole will be adopted. In this paper, the beam optical parameters and their design basis for the STCF storage ring lattice are given. In addition, the preliminary dynamic aperture and beam-beam simulation are studied to get a luminosity more than $0.5 \times 10^{35}\,\mathrm{cm^{-2}s^{-1}}$ at the optimized energy 2 GeV.

KEYWORDS: Accelerator modelling and simulations (multi-particle dynamics; single-particle dynamics); Beam dynamics; Beam Optics

[1] These authors contributed equally to this work.
[*] Corresponding author.

https://doi.org/10.1088/1748-0221/16/07/T07001

2021 JINST 16 T07001

Contents

1 Introduction

High energy physics experiment based on accelerator is one of the most effective ways to study the micro world. Additionally, the accelerator based high luminosity frontier particle physics experiment in the medium energy region is effective for studying flavor physics. In this certain energy region, the high luminosity product will accumulate a large number of data for carrying out high precision measurement, testing the standard model and searching for new physics with high precision [1, 2].

The STCF planning in China, with center mass energy range 2–7 GeV, has the important mission of testing QCD (Quantum Chromo-Dynamics) theory and searching for new physical phenomena beyond the standard model [3]. Moreover, some important physical problems in the Tau-Charm energy region, such as the asymmetry of positive and negative matter in the universe (CP breaking), the internal structure of hadrons and the nature of non-perturbed strong interaction force can be in-depth studied on this facility. Since the high luminosity of the STCF, it can produce more physical events to reduce the statistical error and make some rare production events observable. This STCF is planned to be a double ring electron positron circular collider with 2 A beam current and longitudinally polarized electron beam. The electron and positron beams circulate around two separate rings and intersect at a single Interaction Point (IP) where detector is placed. These two rings have the same lattice structure, except that five Siberian Snakes will be installed in the electron storage ring to get longitudinally polarized beam at the IP.

Additionally, the STCF planning in China will use the latest new collision scheme based on large Piwinski angle and crab waist sextupole to increase luminosity. This novel scheme was proposed in 2006 [4] and has already been experimentally confirmed at DAΦNE, the Italian Φ

2021 JINST 16 T07001

factory in 2010 [5]. The STCF will collide with flat beams, in which case the luminosity can be described as follows [6]

$$L = \frac{\gamma f_0 N_b}{2 r_e \beta_y^*} \xi_y \tag{1.1}$$

where γ is the relativistic factor, f_0 is the collision frequency, r_e is the classical radius of electron, N_b is the number of particles per bunch, β_y^* is the vertical betatron function at the IP and ξ_y is the vertical beam-beam parameter.

From eq. (1.1) we see that the smaller β_y^* the higher luminosity will be. However, due to the hour glass effect, the traditional head-on collision scheme cannot reduce the β_y^* to very small value due to that N_b decreases proportionally for intense beam. Fortunately, the recently proposed large Piwinski angle collision scheme can increase $\frac{N_b}{\beta_y^*}$ by more than one order of magnitude without amplification of the hour-glass effect thus increase the luminosity [7]. The Piwinski angle ϕ, horizontal and vertical beam-beam tune shift ξ_x and ξ_y as well as the half length of interaction beam area L_i are defined as follows

$$\phi = \frac{\sigma_z}{\sigma_x} \tan\theta \approx \frac{\sigma_z}{\sigma_x}\theta \tag{1.2}$$

$$\xi_x = \frac{N_b r_e}{2\pi\gamma} \frac{\beta_x^*}{(\sigma_z \theta)^2} \tag{1.3}$$

$$\xi_y = \frac{N_b r_e}{2\pi\gamma} \frac{\beta_y^*}{\sigma_y \sigma_z \theta} \tag{1.4}$$

$$L_i = \frac{\sigma_z}{\sqrt{1+\phi^2}} \approx \frac{\sigma_x}{\theta} \tag{1.5}$$

where $\sigma_{x,y,z}$ are the RMS beam size, β_x^* is the horizontal betatron function at IP, θ is the half crossing angle. In the large Piwinski angle collision scheme, the synchro-betatron coupling resonances are suppressed by two sextupoles, which are called crab waist sextupoles, located symmetrically on both sides of the IP with certain phase advance and integrated strength. After effectively suppression of the synchro-betatron resonance with crab waist sextupoles the vertical beam-beam parameters ξ_y can be increased with 2–3 times, and then the luminosity will also be improved proportionally. So, large crossing angle is required in this STCF to get a large Piwinski angle and thus reduce the vertical tune shift as well as the beam interaction area [8]. The total crossing angle $2\theta = 60$ mrad is chosen for this design.

Since the luminosity is strongly determined by the lattice optical parameters design, the optical parameters presented in this paper should meet the requirement of large Piwinski angle and crab waist collision scheme. Additionally, there are many restrictive relationships between optical parameters. Thus the following main points should be carefully considered in this design.

(1) Small horizontal beam size and long bunch length are required for increasing Piwinski angle.

(2) The vertical betatron function at the IP should be minimized to about the same size as the half length of the interaction beam area. Namely sub millimeter range of vertical betatron function is required at the IP.

2021 JINST 16 T07001

(3) A pair of crab waist sextupoles will be implemented at a reasonable phase advance from IP with a designed integrated strength. The crab waist sextupoles will rotate the position of the vertical betatron function waist along the axis of the opposite beam to reduce the synchro-betatron resonances.

(4) The tunes of transverse motion should be carefully chosen so as to simultaneously get an acceptable dynamic aperture and beam-beam interaction property that ensure the high luminosity.

The above constraints make it challenging to design the STCF beam parameters. In the following sections, we will give the lattice optical parameters design process with the optimized energy 2 GeV to meet the high luminosity requirement. The lattice design and matching process are based on particle swam algorithm, which has advantages in accurate matching and fast convergence.

2 High luminosity STCF optics design

The total ring is mainly composed of three parts, they are interaction region, arc region and technical region. Each region is designed as the following.

2.1 Interaction region

The crab waist collision scheme requires strong final quadrupole to minimize the vertical betatron function at IP to the order of sub millimeters. Such small vertical betatron function at IP leads to that it grows rapidly in the next section and then causes very large vertical natural chromaticity. The large natural chromaticity will need for strong sextupole magnets to correct it, and thus introduce strong nonlinear effect. In order to reduce the negative effect of sextupoles, local chromaticity correction scheme with minus unity transformation ($-I$ transformation) is employed. With this scheme (if the sextupole length is neglected), the particles with monochromatic momentum are kicked phase-reversely by the same angle at the entrance and exit points of the $-I$ transformation [9]. Then the second sextupole cancels geometrical aberrations caused by the first sextupole and the nonlinear dynamics induced by a pair of sextupoles will be eliminated by each other. As a result, there is no visible effect of their behavior outside the $-I$ transformation [10–12], which is beneficial to nonlinear beam dynamic optimization. The explicit phase constraint combining with very low betatron function at IP and nanoscale emittance cause that the interaction region to be one of the most difficult region for lattice design. We decompose the interaction region into final focus telescope, local chromaticity correction section, crab sextupole section and matching transformation section. Details of each section are given in the following separately.

2.1.1 Final focus telescope

The final focus of collider with crab waist collision scheme is a section to obtain low β^* for realizing high luminosity according to eq. (1.1). The STCF will adopt the in-detector placement of the final focus doublet and solenoids which compensate the effect of the detector longitudinal field on the beam. Two-aperture magnets are used for the final focus doublet and the vacuum chambers are common to the in-coming and out-coming beams. The chromaticity generated by the final focus lens mainly scales according to L^*/β^* , where L^* is the distance from the closest quadrupole to the IP, β^* is the betatron function at the IP [13]. This means the smaller L^* the smaller natural chromaticity will be. But the Machine Detector Interface (MDI) needs a larger L^* for installing compensating solenoid and some chambers. Finally, L^* is set as 0.9 m, which is a compromise between accelerator design and MDI requirement. Following the final focus doublet is the second doublet with a bending magnet separated by a long straight section. In order to reduce the influence of beam-induced background on the detector, the strength of the bending magnet is required to be as weak as possible. However, from the point of local chromaticity correction, the strength of the bending magnet should be strong enough to get a dispersion bump. Overall, the bending magnet beside the final focus doublet is installed at a distance of 5 m from IP, and its strength is 0.107 T at 2 GeV energy. Meanwhile, two doublets interleaved with a bending magnet are used to compose a final focus telescope which satisfies the following matrix

$$M_{x,y} = \begin{pmatrix} F_{x,y} & 0 \\ 0 & 1/F_{x,y} \end{pmatrix} \tag{2.1}$$

where $F_{x,y}$ is a nonzero value, with the subscript x, y denoting horizontal and vertical directions. The merit of the telescope is that the phase advance from IP to the end of the telescope is integer times of π, regardless of how to choose the betatron function at the end of the telescope [13]. The betatron function at the exit of the telescope is only the function of factor $F_{x,y}$ as shown in eq. (2.2).

$$\beta_{x,y}(s_1) = F_{x,y}^2 \beta_{x,y}(s_0) \tag{2.2}$$

This matching work starts from IP. The matrix elements of both transverse planes are the objective function, natural emittance is the constraint function of particle swarm algorithm. By changing the quadrupole strengths and the distance between every magnet, the algorithm can quickly converge to a satisfactory solution space.

2.1.2 Local chromaticity correction section

The chromaticities generated at the final focus lens in the vertical and horizontal planes are $C_y = -169.5$ and $C_x = -7.8$ respectively. Non-interleaved sextupole pairs are adopted for local chromaticity correction as shown in figure 1(a). The chromaticity correction section is composed of a CCY (vertical chromaticity correction) section and a CCX (horizontal chromaticity correction) section. Close to the IP it is the CCY section in which a pair of sextupoles are placed in symmetrical place with high β_y and proper dispersion function. The geometrical center of two sextupoles are spaced with π phase advance in the vertical plane and thus compose a $-I$ transformation, while the phase advance from the final defocusing quadrupole to the first sextupole center of CCY section is $(2\text{m} + 1)\pi$ in the vertical plane, with m an integer [8]. After the CCY section it is the CCX section. In this section two horizontal chromaticity correction sextupoles are also spaced with π phase advance in the horizontal plane, and the horizontal phase advance from the final focusing quadrupole to the first sextupole center of the CCX section is $(2\text{n} + 1)\pi$, with n an integer.

For this process, precisely control of the phase advances between CCX and CCY sextupoles are the main objective functions. The betatron ratio at sextupole magnets and emittance are the constraint functions. After hundreds of iterations the algorithm obtains a satisfactory solution. Result shows that, the betatron ratio at local vertical chromaticity correction sextupole is $\beta_y/\beta_x = 865/2.13$, and dispersion function is 0.13 m. In addition, the betatron ratio at local horizontal

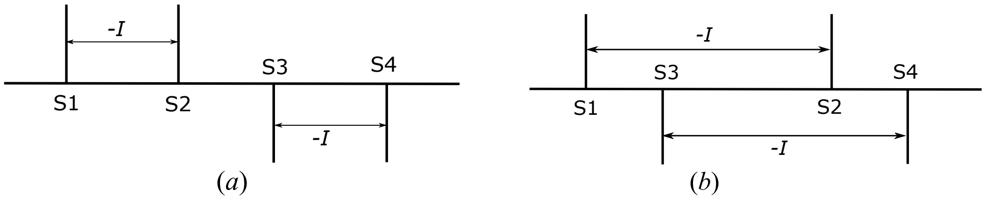

Figure 1. Interleaved and non-interleaved sextupole pair scheme for minus unit transformation. Sub plot (a) is non-interleaved sextupole pair used in the interaction region, (b) is interleaved sextupole pair used in the arc section.

chromaticity correction sextupole is $\beta_x/\beta_y = 41/0.87$, and dispersion function is 0.79 m. The local chromaticity correction sextupole arrangement and the phase advances between them are shown in figure 2.

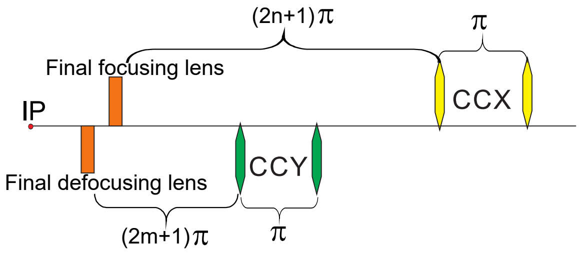

Figure 2. Vertical and horizontal chromaticity correction sections and their phase advances.

2.1.3 Crab sextupole section

Before the crab waist sextupole section, the dispersion function and its derivative are adjusted to zero with a quadrupole and a bending magnet. Then, some quadrupole magnets are arranged to get suitable betatron function and phase advances for crab sextupole implementation. The second order geometrical aberrations can only be eliminated by installing the crab waist sextupoles in location with the horizontal phase advance from IP be k times of π, and the vertical phase advance from IP be $(k' + 0.5)\pi$ as shown in figure 3. The integral strength of the crab sextupole should satisfy,

$$K_2 L = \frac{1}{2\theta\beta_y^*\beta_y}\sqrt{\frac{\beta_x^*}{\beta_x}} \tag{2.3}$$

β_x and β_y are the horizontal and vertical betatron function where crab sextupole is installed. To reduce the strength of the crab waist sextupole the betatron function at crab sextupole position, especially the vertical one needs to be large properly. In our design, the betatron functions at the center of crab sextupole are $\beta_x = 14.52$ m and $\beta_y = 117.8$ m. As a result, the designed integrated crab sextupole strength $K_2L = 18.69\text{m}^{-2}$.

2.1.4 Matching transformation section

At the end of the interaction region some quadrupoles are managed to compose the total interaction region (from IP to the end of the interaction region) to be also a telescope. The telescope scheme

2021 JINST 16 T07001

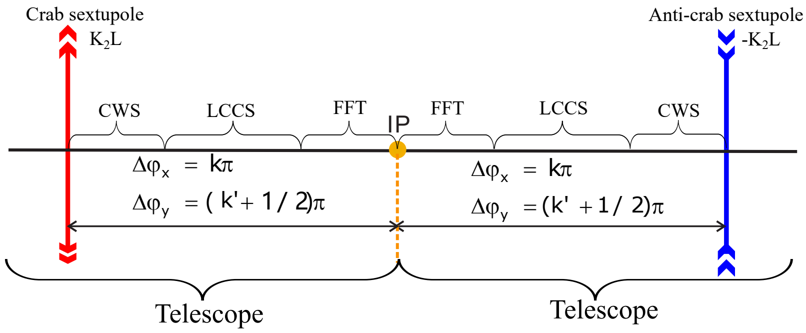

Figure 3. The location of each section from IP, where k and k′ are integer numbers, FFT means final focus telescope, LCCS means local chromaticity correction section, CWS means crab waist sextupole section.

makes the lattice adjustment flexible. Different betatron function at IP can be achieved by changing the matching twiss parameters at the end of the telescope as described in 2.1.1. Besides, the derivative of the betatron function at the end of the telescope is naturally zero. Therefore, as long as the betatron function at the end of the telescope is matched to the arc region, any length of $\pm I$ Siberian Snake (the transverse transformation matrix is I in one direction and $-I$ in the other direction) can be added at the end of the interaction region.

The bending angle of half interaction region is 36 degrees, so that two Siberian Snakes can be installed on both sides of the interaction region. The optical function of a half interaction region satisfying the above requirements are shown in figure 4. Phase advance of the interaction region is shown in figure 5.

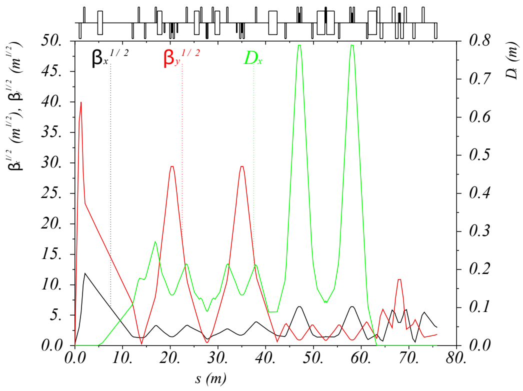

Figure 4. Optical function of half interaction region.

2.2 Bending arc region

This region is designed for getting a satisfactory beam emittance, bunch length, energy spread to improve the requirement of large Piwinski angle and crab waist collision, as well as getting a reasonable geometrical bending. In this design the seven-bend achromatic arc region is chosen. Since the electron ring will install 5 Siberian Snakes to get high longitudinally polarized beam at the IP, each of the arc cell will bend 36 degrees so that Siberian Snakes can be installed at equal azimuth [14]. Getting low emittance at the arc region and arranging chromaticity correction

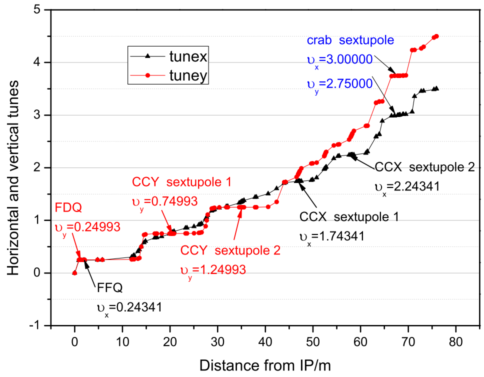

Figure 5. Phase advance of half interaction region.

sextupoles to get large enough dynamic aperture is another point worth noting. Design of this arc section is independent of the interaction region. By constructing reasonable objective functions and constraints the particle swarm optimization algorithm can search for satisfactory arc section. In this design two dispersion bumps are created to install chromatic sextupoles. The phase advance between the two dispersion bumps are 3π in the horizontal plane and π in the vertical plane. And then the interleaved sextupole pair scheme with $-I$ transformation can be installed in the dispersion bumps (as shown in figure 1(b)). Five-bend achromatic arc cell is also tested in our design, but this structure is hard to get the satisfactory horizontal phase advance with proper beam emittance. Namely, the horizontal phase advance often greater than π and less than 3π.

The dispersion suppressor at the two sides of the arc section is a simple doublet structure. The doublet dispersion suppressor will match the horizontal dispersion function and its derivative to zero. After the dispersion suppressor it is a triplet matching section. One side of the arc is matched with a triplet to a 5 m long straight section, and the other side is matched with a triplet to the end of the interaction region. Siberian Snake can be placed between the triplet and matching transformation of interaction region. One super-period of the arc section is shown in figure 6.

2.3 Technical region

The technical section is placed at the opposite side of the interaction region. This section is a 61.95 m long straight section with many quadrupole magnets. It is designed for top-up injection, RF cavity installation, ring separation, Siberian Snake installation, tune adjustment for high luminosity and large dynamic aperture, as well as other insertion devices installation.

3 Design result and total ring

Summarizing the above design, the total ring is composed of eight bending arc periods (four super-periods), one interaction region, one technical region and five Siberian snakes. General layout of the STCF storage ring is shown in figure 7. The beam and machine parameters calculated by ELEGANT code [16] are listed in table 1. The Touschek life tracking result is also given in this table.

2021 JINST 16 T07001

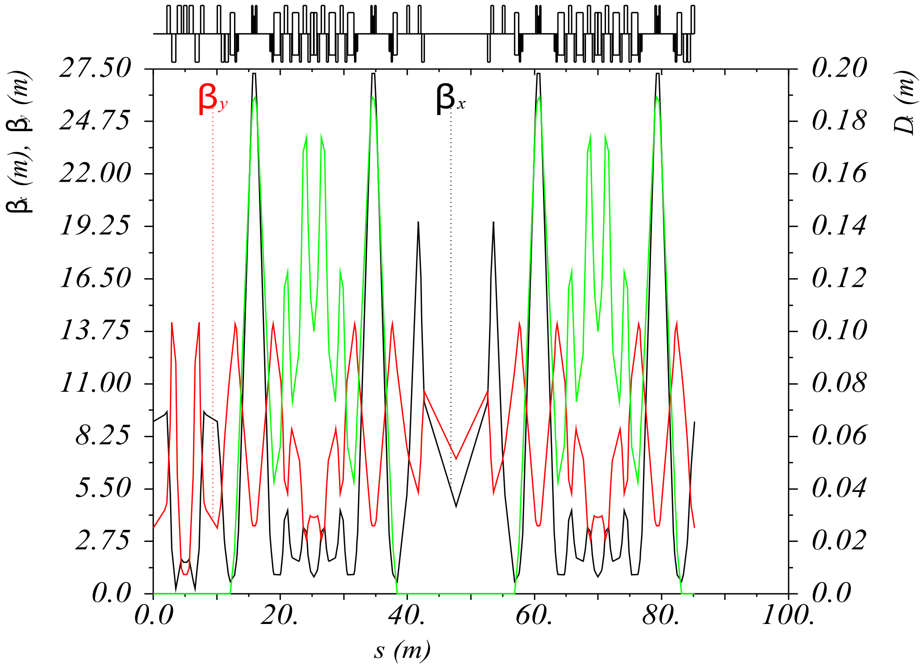

Figure 6. One super-period of the arc region, left side is a Siberian Snake, at the mid of one-super period is a 10 m long straight section for damping wiggler implementation.

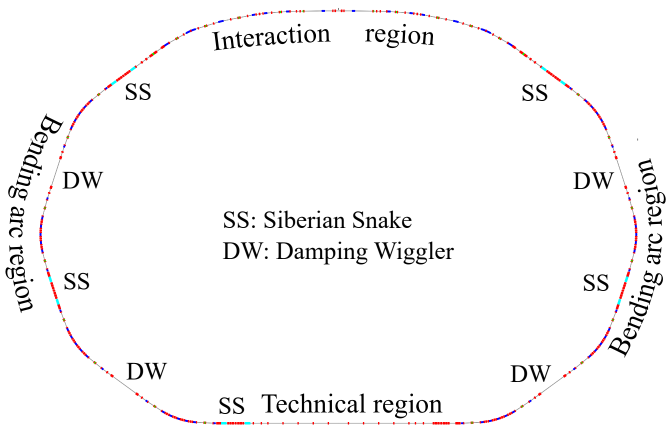

Figure 7. General geometry of STCF storage ring.

Except the linear optics design, the STCF collider must have enough dynamic aperture to store the colliding beam. In particular, the dynamic momentum acceptance must be large enough to guarantee a sufficiently long beam lifetime. A particle swarm algorithm based optimization code developed by our research group is used for nonlinear dynamic optimization and ELEGANT code is used for checking the dynamic aperture tracking result.

Research shows that the choice of working point has an important influence on the dynamic aperture and the stability of luminosity. By adjusting the technical section, we set the working points to $\nu_x = 33.567$, $\nu_y = 20.606$, and the corresponding dynamic aperture is optimized. We use 28 groups (5 kinds of strength) of chromaticity sextupoles which installed at the position with $-I$ transformation

Table 1. Key parameters of the STCF.

Parameters	Unit	Value
Circumference	m	574.78
Distance from final defocusing quadrupole to IP	m	0.9
Optimized energy	GeV	2.0
Total beam current	A	2
Horizontal/Vertical beta @ IP	m	0.09/0.0006
Total crossing angle (2θ)	mrad	60
Piwinski angle (ϕ)	rad	18.9
Beam-beam tune shift (ξ_x/ξ_y)	—	0.0038/0.0835
Coupling ratio	—	0.5%
Natural chromaticities (C_x/C_y)	—	-87/-513
Horizontal emittance (ϵ_x) without/with IBS	nmrad	2.76/4.17
Horizontal beam size @ IP without/with IBS	µm	15.77/19.37
Vertical beam size @ IP without/with IBS	µm	0.091/0.117
Energy spread ($\frac{\sigma_{\Delta E}}{E}$) without/with IBS	$\times 10^{-4}$	5.3/7.2
Momentum compaction factor	—	7.2×10^{-4}
RF frequency	MHz	499.67268
RF voltage	MV	1.2
Harmonic number	—	958
Bunch length (σ_z)	mm	12.2
Particle number per bunch (N_b)	—	5.0×10^{10}
Energy loss per turn	MeV	0.1315
Synchrotron tune (ν_s)	—	0.00388
Damping times ($\tau_x/\tau_y/\tau_s$)	ms	58.51/58.33/29.12
Peak luminosity	$cm^{-2}s^{-1}$	1.2×10^{35}
Touschek lifetime	s	35

as that reserved in the previous linear optics design. But, the result shows that it is hard to get large enought off-momentum dynamic aperture simply with the $-I$ transformation sextupoles. For this reason we add two families of sextupoles in the interaction region to enlarge the on/off-momentum aperture. By optimizing these sextupole pairs a preliminary dynamic aperture tracked 3000 turns with ELEGANT code is shown in figure 8. Also, the dynamic aperture with momentum deviation is given in figure 9. In the above simulations the solenoids of Siberian Snakes are turned off.

A preliminary beam-beam simulation is also carried out with a three-dimensional strong-strong PIC code developed by Beijing Electron-Positron Collider (BEPC) [15]. The beam-beam interaction simulation shows that the luminosity has a better stability with the fractional part of tune in the vertical plane larger than the horizontal one. The luminosity simulation result with the above tune is given in figure 10. The results show that the luminosity tends to be stable after 10,000 turns, and the final balanced luminosity can reach to $0.72 \times 10^{35}\ cm^{-2}s^{-1}$.

2021 JINST 16 T07001

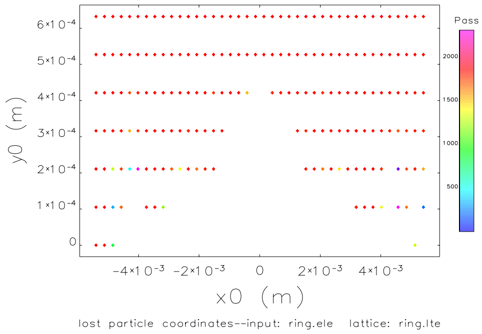

Figure 8. The dynamic aperture at injection point, corresponding tune 33.567/20.606. The maximum aperture is $21\sigma_x$ in the horizontal plane and $45\sigma_y$ in the vertical plane.

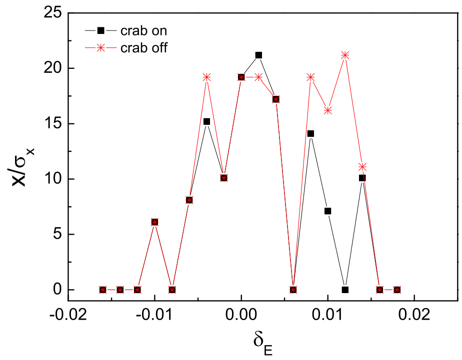

Figure 9. The horizontal aperture with momentum deviations.

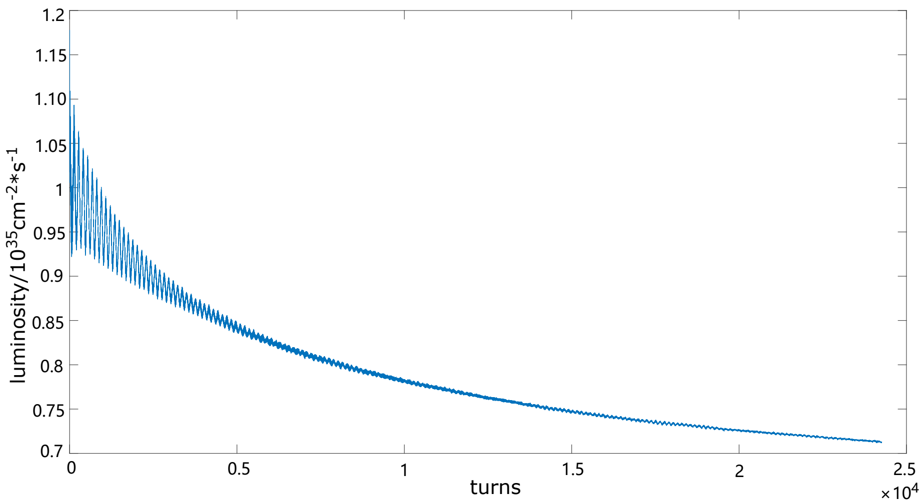

Figure 10. The luminosity simulation by strong-strong interaction, corresponds to tune 33.567/20.606.

4 Summary and outlook

In conclusion, design basics and some results of a STCF lattice are given in this paper. Linear lattice is designed with considering many factors and high precision to meet the high luminosity. The traditional method of $-I$ transformation for improving the nonlinear beam dynamic are carefully applied both in interaction region and bending arc region, however displays an unsatisfactory result. By adding other sextupoles in interaction region, finally, on and off-momentum dynamic aperture are improved obviously although the latter still has some defects. In the next work, the higher order chromaticities and the tune shift due to the finite length of the main sextupoles should be further corrected, as well as tune scan should be implemented in detail to find out better dynamic aperture and higher luminosity. Other issues such as instabilities and polarization will be further optimized in the following work.

Acknowledgments

This work is supported by the Natural Science Foundation of Fujian Province (grant number 2018J01586), the National Natural Science Foundation of China (grand number 12005039), Fujian Education Department Fund (grant number JAT190435), Scientific Research Starting Foundation of Fujian University of Technology (grand numbers GY-Z14080 and GY-Z14081). This work is also supported by the Double First-Class University Project Foundation of USTC (Key Technology R&D for Super Tau-Charm Facility).

References

[1] LHCb collaboration, *B flavour tagging using charm decays at the LHCb experiment*, 2015 *JINST* **10** P10005 [arXiv:1507.07892].

[2] LHCb collaboration, *Measurement of CP violation in $B^0 \to J/\psi K^0_S$ decays*, *Phys. Rev. Lett.* **115** (2015) 031601 [arXiv:1503.07089].

[3] G. S. Huang et al., *Physics on the high intensive electron position accelerator at 2–7 GeV*, *Chin. Sci. Bull.* **62** (2017) 1226 (in Chinese).

[4] P. Raimondi, *Status on Super-B Effort*, *Conf. Proc. C* **0606141** (2006) 104.

[5] M. Zobov et al., *Test of crab-waist collisions at DAFNE Phi factory*, *Phys. Rev. Lett.* **104** (2010) 174801.

[6] E. Levichev, *The project of a Tau-Charm factory with crab waist in Novosibirsk*, *Phys. Part. Nucl. Lett.* **5** (2008) 554.

[7] P. Raimondi, D. Shatilov and M. Zobov, *Beam-beam issues for colliding schemes with large piwinski angle and crabbed waist*, DOI: 10.15161/oar.it/1449009600.96.

[8] A. Bogomyagkov, E. Levichev and P. Piminov, *Final focus designs for crab waist colliders*, *Phys. Rev. Accel. Beams* **19** (2016) 121005.

[9] K.L. Brown, *First-and second-order charged particle optics*, SLAC-PUB-3381 (1984).

[10] Y. Wang, F. Su, S. Bai, Y. Zhang, T. Bian, D. Wang et al., *Lattice design for the CEPC double ring scheme*, *Int. J. Mod. Phys. A* **33** (2018) 1840001.

2021 JINST 16 T07001

[11] K.L. Brown, *Basic optics of the SLC final focus system*, SLAC-PUB-4811 (1988).

[12] K. Oide et al., *Design of beam optics for the Future Circular Collider e^+e^--collider rings*, *Phys. Rev. Accel. Beams* **19** (2016) 111005 [*Addendum ibid.* **20** (2017) 049901] [arXiv:1610.07170].

[13] Y. Cai, *Analytical approach to chromatic correction in the final focus system of circular colliders*, *Phys. Rev. Accel. Beams* **19** (2016) 111006.

[14] E.D. Courant, *Accelerators, Colliders, and Snakes*, *Ann. Rev. Nucl. Part. Sci.* **53** (2003) 1.

[15] Y. Zhang, K. Ohmi and L.-M. Chen, *Simulation study of beam-beam effects*, *Phys. Rev. ST Accel. Beams* **8** (2005) 074402.

[16] M. Borland et al., *User's Manual for elegant*, *Program version 29.1.0* (2016).

2021 JINST 16 T07001